Available online at www.sciencedirect.com
ScienceDirect
Scripta Materialia 61 (2009) 1149–1152
Scripta MATERIALIA
www.elsevier.com/locate/scriptamat

Effect of Y-junction nanotubes on strengthening of nanocomposites

M.Yu. Gutkin* and I.A. Ovid'ko

Institute of Problems of Mechanical Engineering, Russian Academy of Sciences, Bolshoj 61, Vasilievskii Ostrov, St. Petersburg 199178, Russia

Received 30 July 2009; revised 23 August 2009; accepted 23 August 2009
Available online 27 August 2009

A dislocation model is proposed which describes the strengthening effect of Y-junction nanotubes in nanocomposites. In the model, nanotubes slip along the nanotube/matrix interface through the motion of prismatic dislocation loops. When such a loop meets a Y-junction of nanotubes, it needs a critical shear stress to bypass the junction. It is shown that the critical stress increases with decreasing nanotube radius and wall thickness. Thus, the thinnest nanotubes should provide the most effective strengthening and toughening of such nanocomposites.

Keywords: Nanocomposite; Nanotubes; Dislocations; Interface defects; Plastic deformation

Ceramic nanocomposite bulk materials and coatings showing outstanding mechanical properties (superstrength, superhardness, good wear resistance) have been the subject of rapidly growing research efforts (e.g. [1–8]). In particular, in the last decade, a new generation of advanced nanocomposites reinforced by carbon nanotubes (CNTs) has been fabricated for a range of potential applications [9,10]. CNTs have been embedded into metallic [11–16] and ceramic [10,17–23] matrices, and this process has resulted in significant enhancements to their mechanical properties such as hardness [10,12,15,22,23], strength [10–18], Young's modulus [11,13,14,23], fracture toughness [10,17–22] and wear resistance [10,15,23]. The very large increments (up to 300%) in toughness shown by several CNT – ceramic nanocomposites [19–21] have greatly stimulated interest in understanding micromechanisms which hamper crack growth. The well-known reinforcement mechanisms of CNTs are CNT pulling-out, CNT rupture, bridging and crack deflection [18]. Balani et al. [22] have paid special attention to multidirectional CNT bridges and anchors, CNT – ceramic interface and Y-junction CNTs. Y-junction CNTs are representatives of a large variety of branched nanotubes (C [24–27], CN_x [28], Al_2O_3 [29], etc.) which are produced mainly for nanodevice applications. We believe that it might also be possible to exploit Y-junction CNTs as strengthening elements of nanocomposites. Due to their complex shape, such CNTs are expected to be more effective than their conventional straight counterparts. The main aim of this paper is to theoretically describe the strengthening effect of Y-junction nanotubes (in particular, CNTs) in nanocomposites.

Consider a simplified elastic model of a Y-junction nanotube as a T-like junction of two hollow tubes embedded to an elastic matrix (Fig. 1). Suppose that the tube and matrix materials are elastically isotropic and have different shear moduli (G_1 and G_2) and Poisson ratios (ν_1 and ν_2). The tubes have identical cross-sections of outer radius R and the same wall thickness h. The outer surfaces of the tubes are in coherent contact with the matrix, while their inner surfaces are free of stresses. We will use the Cartesian coordinates with the origin on the axis of the "vertical" tube (the y-axis) and with the x-axis lying along the bottom line of the "horizontal" tube surface.

Let the "vertical" tube be subject to an axial force which tries to pull the tube out of the matrix during the process of deformation or fracture of such a system. Under the action of this force, a shear stress τ appears at the interface between the "vertical" tube and the matrix far from the tube junction (Fig. 1). This shear stress can relax through the mechanism of nucleation of a circular prismatic dislocation loop with Burgers vector **b**, which glides along the interface [30,31]. The Burgers vector **b** can either be a vector of the matrix lattice, if the lattice is properly oriented with respect to the tube axis, or a vector of relative interfacial shear conserving the

* Corresponding author. E-mail: gutkin@def.ipme.ru

1359-6462/$ - see front matter © 2009 Acta Materialia Inc. Published by Elsevier Ltd. All rights reserved.
doi:10.1016/j.scriptamat.2009.08.032

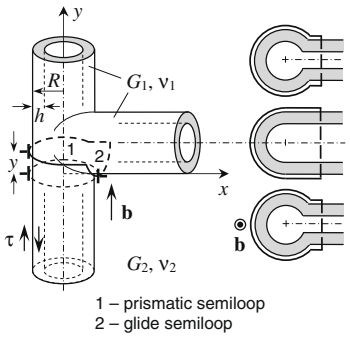

Figure 1. Circular prismatic dislocation loop (the closed dashed line at $y = 0$) with Burgers vector **b** bypasses a Y-junction of nanotubes by a mechanism of loop transformation to two semi-loops: (1) prismatic and (2) glide ones. On the right-hand side, the cross-sections show the changes in the configuration of prismatic semi-loop 1 at the points $h < y < R$, $y = R$, and $R < y < 2R - h$ (from bottom to top).

tube–matrix interface crystallography, in which case we deal with interface dislocation. Within our continual approach, these two cases differ by only the Burgers vector magnitude b. However, our results will always be normalized by b. Therefore, hereinafter we do not differentiate between these cases. In any case, the tube junction is an obstacle to the dislocation glide. To overcome this obstacle and glide further, the dislocation loop must first transform from a planar circle to a complex spatial loop, which bypasses the surface parts of both the tubes in the junction, and then to two closed circular loops, the prismatic one around the "vertical" tube and the glide one around the "horizontal" tube. After that, the new prismatic loop can glide further along the "vertical" tube, while the new glide loop becomes an additional obstacle for subsequent prismatic loops gliding along the "vertical" tube. This mechanism of bypassing the tube junction is similar to the Orowan mechanism of dislocation bypass of precipitates in alloys and particles in disperse composites.

Consider the conditions necessary for activation of the proposed mechanism. This can be done through investigation of the change in the system energy with evolution of the shape of the dislocation loop (Fig. 1). A rigorous solution of this problem is hardly possible, so we will use the approximation of linear tension. This approximation seems to be correct if the tube wall thickness is much smaller than the tube radius: $h << R$. In this case, the inside free surface of the tube is very close to the dislocation line and provides a stronger screening effect on the dislocation elastic fields compared to that of the dislocation loop shape [30,31]. Therefore, to estimate the dislocation strain energy, we can use a greatly simplified planar model of a straight dislocation in the interface between a semi-infinite substrate (matrix) and a thin layer (tube wall).

In the initial state, when the prismatic dislocation loop is pushed to the tube junction and lies in the plane $y = 0$ (see the dashed circle in Fig. 1), its energy can be written as:

$$W_0 = 2\pi R b^2 (w_{e1} + \bar{D}), \tag{1}$$

where b is the Burgers vector magnitude of the dislocation loop, and $b^2 w_{e1}$ and $b^2 \bar{D}$ are the strain and core energies, respectively, per unit length of a straight edge dislocation with the Burgers vector lying in the substrate–layer interface. The term w_{e1} can be obtained from the solution [32,33] for an edge dislocation in a thin two-layer plate in the limiting case where the thickness of one layer tends to infinity. After some algebra, we have:

$$w_{e1} = D_1 \left\{ \frac{2 - A - B}{2} \ln\frac{h}{b} + \int_0^{+\infty} \frac{e^{-hs}}{sp(s)} \left[f_{y1}(s) g_{y1}(s) + f_{y2}(s) g_{y2}(s) \right] \mathrm{d}s \right\}, \tag{2}$$

where $D_i = G_i/[\pi(k_i + 1)]$, $k_i = 3 - 4\nu_i$, $i = 1, 2$, $A = (1 - \Gamma)/(1 + k_1\Gamma)$, $B = (k_2 - k_1\Gamma)/(k_2 + \Gamma)$, $\Gamma = G_2/G_1$, $f_{y1}(s) = -(1 - A)hs + (A - B)/2 + E[A(1 - B)hs - (A - B)/2]$, $f_{y2}(s) = (1 - A)hs - (2 - A - B)/2 + E[A(1 - B)hs - AB + (A + B)/2]$, $g_{y1}(s) = E_-(h - b)s + E_+[2Ahbs^2 - A(h - b)s - (A - B)/2] - E[2Ah^2s^2 - (A - B)/2]$, $g_{y2}(s) = -1 + E_-[1 - (h - b)s] - E_+[2Ahbs^2 - A(h + b)s + (A + B)/2] + E[2Ah^2s^2 - 2Ahs + (A + B)/2]$, $p(s) = 1 - 2E[2Ah^2s^2 + (A + B)/2] + E^2AB$, $E = \exp(-2hs)$, $E_- = \exp[-(h - b)s]$, and $E_+ = \exp[-(h + b)s]$. The term $\bar{D}$ can be estimated [30,31] by $\bar{D} = (D_1 + D_2)/2 = D_1[1 + \Gamma(1 - \nu_1)/(1 - \nu_2)]/2$.

The energy of the spatial dislocation loop, which consists of prismatic semi-loop 1 lying in the plane $0 < y < 2R$ and glide semi-loop 2 formed in the plane $x = R$ around the "horizontal" tube, is given by the sum $W(y) = W_1(y) + W_2(y)$, where the first term is the energy of semi-loop 1 and the second term is the energy of semi-loop 2. The first term is approximated by:

$$W_1(y) = b^2 L_1(y)(w_{e1} + \bar{D}), \tag{3}$$

where $L_1(y)$ is the length of semi-loop 1. As follows from geometry of the y-section of the tube junction (Fig. 1), this length reads $L_1(y) = (2 + \pi)R - 2|R - y| + 2R \arcsin(|R - y|/R)$. It is easy to find that $L_1(0) = L_1(2R) = 2\pi R$ and $W_1(0) = W_1(2R) \equiv W_0$. In the center of the tube junction, at $y = R$, the length of semi-loop 1 is minimal, $L_1(R) = (2 + \pi)R$.

In calculating the second term, $W_2(y)$, one must take into account that semi-loop 2 is the line of mixed-type dislocation with variable edge and screw components. Within the line-tension approach, the integration of the corresponding contributions to the dislocation energy over the length of semi-loop 2 results in:

$$W_2(y) = Rb^2[(w_{e2} + \bar{D})(P - Q) + (w_s + \bar{G})(P + Q)]. \tag{4}$$

Here $b^2 w_{e2}$ and $b^2 \bar{D}$ are the strain and core energies, respectively, per unit length of a straight edge dislocation with the Burgers vector normal to the substrate–layer interface; $b^2 w_s$ and $b^2 \bar{G}$ are the strain and core energies, respectively, per unit length of a screw dislocation lying in the substrate–layer interface; $P = \pi/2 + \arcsin(y/R - 1)$, $Q = (y/R - 1)\sqrt{y/R}\ \sqrt{2 - y/R}$, and $\bar{G} = (G_1 + G_2)/(8\pi)$.

The term w_{e2} can be found in a similar way as w_{e1}, by limiting transition from the solution [32,33], which gives:

$$w_{e2} = D_1\left\{\frac{2-A-B}{2}\ln\frac{h}{b} - \int_0^{+\infty}\frac{e^{-hs}}{sp(s)}[f_{x1}(s)g_{x1}(s) + f_{x2}(s)g_{x2}(s)]\mathrm{d}s\right\} \quad (5)$$

with $f_{x1}(s) = 1 + (1-A)hs - (A+B)/2 + E[A(1-B)hs + AB - (A+B)/2]$, $f_{x2}(s) = (1-A)hs + (A-B)/2 - E[A(1-B)hs + (A-B)/2]$, $g_{x1}(s) = -1 + E_-[1 + (h-b)s] - E_+[2Ahbs^2 + A(h+b)s + (A+B)/2] + E[2Ah^2s^2 + (A+B)/2]$, $g_{x2}(s) = E_-(h-b)s - E_+[2Ahbs^2 + A(h-b)s - (A-B)/2] + E[2Ah^2s^2 - (A-B)/2]$, and $p(s)$, E, E_- and E_+ being the same as in Eq. (2).

To calculate the screw dislocation strain energy b^2w_s, one can use the approach of infinite series of image dislocations as suggested in Ref. [34]. Omitting the intermediate calculations, we obtain the final result:

$$w_s = \frac{G_1}{4\pi}\left\{\ln\frac{2h-b}{b} + \sum_{n=1}^{\infty}\left(\frac{1-\Gamma}{1+\Gamma}\right)^n \ln\frac{4h^2n^2-(2h-b)^2}{4h^2n^2-b^2}\right\}. \quad (6)$$

Thus, the sum energy $W(y) = W_1(y) + W_2(y)$ of the spatial dislocation loop is determined by Eqs. (3)–(6). The energy change due to the transformation of the planar prismatic dislocation loop into the complex spatial dislocation loop, which consists of prismatic semi-loop 1 and glide semi-loop 2 (Fig. 1), is then given by:

$$\Delta W(y) = W(y) - W_0 - A(y), \quad (7)$$

where A is the work done by the applied shear stress τ to shift the prismatic semi-loop 1 from the point $y = 0$ to the point y. Neglecting the local change of the stress τ near the tube junction, we can approximate this work by $A(y) \approx 2\pi Rby\tau$.

Consider the energy change given by Eq. (7) in dependence on y, for different values of τ. In the majority of nanocomposites reinforced by nanotubes, the nanotubes are much harder than the matrix, so we take $\Gamma = G_2/G_1 = 0.1$. We also put $\nu_1 = \nu_2 = 0.3$ for definiteness. As an exemplary case, we consider a Y-junction of very thin nanotubes with the outer radius $R = 15b$ and the wall thickness $h = 2b$, which can serve as a first-order-approximation model for the Y-junction of single-wall carbon nanotubes (SWCNs).

The curves $\Delta W(y)$ are plotted in Figure 2, for the stress values ranging from $\tau = 0$ to $\tau = 16G_1/1000$. Here the initial value of the y-coordinate is the elementary shift of semi-loop 1 by one atomic spacing b, i.e. $y/R = 0.067$. It is seen from Figure 2 that under a small value of τ (here at $\tau = 0$), the energy change ΔW is positive for any y. This means that a prismatic dislocation loop cannot bypass the Y-junction of nanotubes under such a low stress. Under a moderate value of τ (here at $\tau = (4\ldots10)G_1/1000$), ΔW is positive for small, but negative for large values of y (Fig. 2a). Therefore, to bypass the Y-junction, the loop must overcome an energy barrier of the height smaller or about $0.02G_1b^2R = 0.3G_1b^3$. Under higher values of τ, this energy barrier disappears, the energy change ΔW becomes negative for any y and monotonously decreases until its minimum near $y = 2R$ (Fig. 2b). In this case, the dislocation loop freely bypasses the Y-junction by the mechanism under discussion.

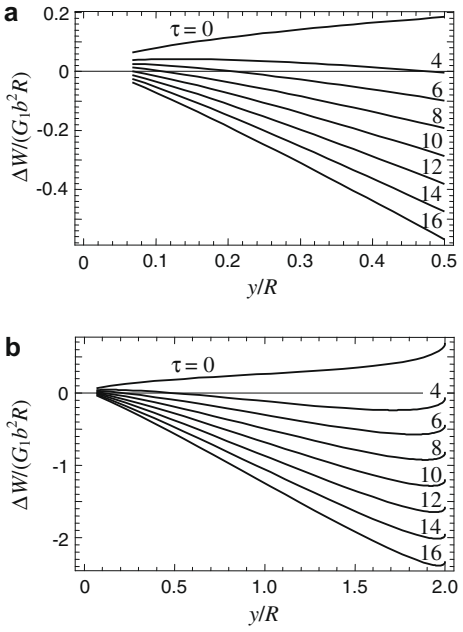

Figure 2. Dependence of the energy change ΔW on the normalized path y/R of prismatic semi-loop 1 at the initial (a) and the whole (b) region of the Y-junction at $\Gamma = 0.1$, $R = 15b$, and $h = 2b$. The values of the applied shear stress τ are given at curves in units of $G_1/1000$.

The critical stress value $\tau = \tau_c$, at which the barrierless bypass becomes energetically favorable, is determined in this case by the necessary condition $\Delta W(y = b) = 0$ that immediately gives:

$$\tau_c = \frac{W(y=b) - W_0}{2\pi Rb^2}. \quad (8)$$

The dependence $\tau_c(R/b)$ is shown in Figure 3, for different values of the nanotube wall thickness h. The critical stress τ_c fast decreases with an increase in the nanotube radius R in the range of relatively small R (here at R smaller or about $200b \approx 60$ nm for $b \approx 0.3$ nm) and slowly decreases with R in the range of larger R. The critical stress values are not too high; for $R = 50b \approx 15$ nm, it varies from $G_1/200$ to $G_1/189$ depending on the wall thickness h. In the limiting case of an extremely thin nanotube of radius $R = 10b \approx 3$ nm and wall thickness $h = 2b \approx 0.6$ nm, where our con-

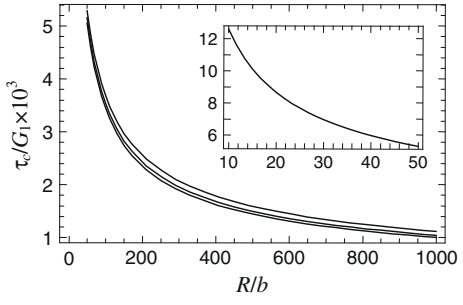

Figure 3. Dependence of the critical shear stress τ_c on the normalized nanotube radius R/b for $\Gamma = 0.1$ and different values of the normalized nanotube wall thickness: $h/b = 2$, 5 and 10 (from top to bottom). The inset demonstrates the same dependence at $\Gamma = 0.1$ and $h/b = 2$ in the range of relatively small values of R/b.

tinuum approach is still correct, the critical stress is already rather high, $\tau_c \approx G_1/79$ (see the inset in Fig. 3).

The interesting and unusual result is the increase of τ_c with a decrease in the wall thickness h. On the first sight, one can expect an inverse dependence because the energy of dislocation loop increases with h. However, as we have carefully checked, the energy change ΔW is not a monotonic function of h (the corresponding plots are not shown here); first, it increases with h and reaches its maximum at $h = 2b$, and after it decreases with h. As a corollary, the critical stress τ_c decreases with h, too, although this dependence is rather weak (Fig. 3).

In summary, we have proposed a dislocation model to describe the strengthening effect of Y-junction nanotubes in nanocomposites. Within the model, the nanotube glides along the nanotube–matrix interface through generation and slip of prismatic dislocation loops. When such a loop meets a Y-junction of nanotubes, it needs a critical shear stress to bypass the junction via a loop transformation mechanism. The critical stress value increases with decreasing radius and wall thickness of the nanotubes. Therefore, the thinnest nanotubes like SWCNs are expected to provide the most effective strengthening and toughening of such nanocomposites. This conclusion is in agreement with the experimental results reported in Refs. [19–21].

The work was supported, in part, by the Russian Foundation of Basic Research (Grants 08-01-00225-a and 08-02-00304-a), the National Science Foundation (Grant CMMI no. 0700272), Office of Naval Research (Grant N00014-07-1-0295), and Russian Academy of Sciences Program "Fundamental studies in nanotechnologies and nanomaterials".

[1] J.A. Vreeling, V. Ocelik, G.A. Hamstra, Y.T. Pei, J.Th.M. De Hosson, Scr. Mater. 42 (2000) 589.
[2] C. Strondl, G.J. van der Kolk, T. Hurkmans, W. Fleischer, T. Trinh, N.M. Carvalho, J.T.M. De Hosson, Surf. Coat. Technol. 142–144 (2001) 707.
[3] S. Veprek, Rev. Adv. Mater. Sci. 5 (2003) 6.
[4] S.C. Tjong, H. Chen, Mater. Sci. Eng. R 45 (2004) 1.
[5] S. Zhang, D. Sun, Y. Fu, Y.T. Pei, J.Th.M. De Hosson, Surf. Coat. Technol. 200 (2005) 1530.
[6] D. Galvan, Y.T. Pei, J.Th.M. De Hosson, Surf. Coat. Technol. 200 (2006) 6718.
[7] A. Mukhopadhyay, B. Basu, Int. Mater. Rev. 52 (2007) 257.
[8] C.C. Koch, I.A. Ovid'ko, S. Seal, S. Veprek, Structural Nanocrystalline Materials: Fundamentals and Applications, Cambridge University Press, Cambridge, 2007.
[9] E.T. Thostenson, Z. Ren, T.W. Chou, Compos. Sci. Technol. 61 (2001) 1899.
[10] J. Cho, A.R. Boccaccini, M.S.P. Shaffer, J. Mater. Sci. 44 (2009) 1934.
[11] S.I. Cha, K.T. Kim, S.N. Arshad, C.B. Mo, S.H. Hong, Adv. Mater. 17 (2005) 1377.
[12] Y. Feng, H.L. Yuan, M. Zhang, Mater. Charact. 55 (2005) 211.
[13] R. George, K.T. Kashyap, R. Rahul, S. Yamdayni, Scr. Mater. 53 (2005) 1159.
[14] H.J. Choi, G.B. Kwon, G.Y. Lee, D.H. Bae, Scr. Mater. 59 (2008) 360.
[15] P.Q. Dai, W.C. Xu, Q.Y. Huang, Mater. Sci. Eng. A 483–484 (2008) 172.
[16] J. Kang, P. Nash, J. Li, C. Shi, N. Zhao, Nanotechnology 20 (2009) 235607.
[17] R.Z. Ma, J. Wu, B.Q. Wei, J. Liang, D.H. Wu, J. Mater. Sci. 33 (1998) 5243.
[18] J. Ning, J. Zhang, Y. Pan, J. Guo, Mater. Sci. Eng. A 357 (2003) 392.
[19] G.D. Zhan, J.D. Kuntz, J. Wan, A.K. Mukherjee, Nat. Mater. 2 (2003) 38.
[20] J.D. Kuntz, G.D. Zhan, A.K. Mukherjee, MRS Bull. 29 (2004) 22.
[21] G.D. Zhan, A.K. Mukherjee, Rev. Adv. Mater. Sci. 10 (2005) 185.
[22] K. Balani, T. Zhang, A. Karakoti, W.Z. Li, S. Seal, A. Agarwal, Acta Mater. 56 (2008) 571.
[23] V. Singh, R. Diaz, K. Balani, A. Agarwal, S. Seal, Acta Mater. 57 (2009) 335.
[24] J. Li, G. Papadopulos, J. Xu, Nature 402 (1999) 253.
[25] B.O. Satishkumar, P.J. Thomas, A. Govindaraj, C.N.R. Rao, Appl. Phys. Lett. 77 (2000) 2530.
[26] M. Terrones, F. Banhart, N. Grobert, J.-C. Charlier, H. Terrones, P.M. Ajayan, Phys. Rev. Lett. 89 (2002) 075505.
[27] J.M. Ting, C.C. Chang, Appl. Phys. Lett. 80 (2002) 324.
[28] P. Ghosh, M. Subramanian, R.A. Afre, M. Zamri, T. Soga, T. Jimbo, V. Filip, M. Tanemura, Appl. Surf. Sci. 255 (2009) 4611.
[29] J. Zou, L. Pu, X. Bao, D. Feng, Appl. Phys. Lett. 80 (2002) 1079.
[30] M.Yu. Gutkin, I.A. Ovid'ko, Scr. Mater. 59 (2008) 414.
[31] M.Yu. Gutkin, I.A. Ovid'ko, Phys. Solid State 50 (2008) 2053.
[32] M.Yu. Gutkin, A.E. Romanov, Phys. Status Solidi A 125 (1991) 107.
[33] M.Yu. Gutkin, A.E. Romanov, Phys. Status Solidi A 129 (1992) 363.
[34] M.L. Öveçoğlu, M.F. Doerner, W.D. Nix, Acta Metall. 35 (1987) 2947.